Direct measurement of the masses of ^{11}Li and $^{26-32}$Na with an on-line mass spectrometer

C. Thibault, R. Klapisch, C. Rigaud, A. M. Poskanzer,* R. Prieels,† L. Lessard,‡ and W. Reisdorf§
Laboratoire René Bernas du Centre de Spectrométrie Nucléaire et de Spectrométrie de Masse, 91406 Orsay, France
(Received 17 March 1975)

The use of an on-line mass spectrometer to make direct mass measurements of short-lived isotopes far from the stability line has been improved to yield more accurate mass measurements for $^{27-30}$Na, new mass measurements for ^{11}Li, ^{31,32}Na, and to remove a discrepancy between existing mass measurements of ^{26}Na. The mass excesses (keV) measured are: ^{11}Li, 40940 ± 80; ^{26}Na, −6901 ± 25; ^{27}Na, −5620 ± 60; ^{28}Na, −1140 ± 80; ^{29}Na, 2650 ± 100; ^{30}Na, 8370 ± 200; ^{31}Na, 10600 ± 800; ^{32}Na, 16400 ± 1100. The ^{11}Li value indicates that it is bound by only 170 ± 80 keV. The masses of ^{31}Na and ^{32}Na imply that these nuclei are more tightly bound than expected from theoretical predictions.

[NUCLEAR STRUCTURE ^{11}Li, $^{26-32}$Na; measured atomic masses. On-line mass spectrometer.
RADIOACTIVITY ^{11}Li; deduced logft.]

I. INTRODUCTION

The possibility of producing light nuclei with a large neutron excess by reactions of high energy protons with heavy targets[1,2] or in complex transfer reactions induced by heavy ions,[3] has been at the origin of a considerable new interest in the field of light exotic nuclei. For some nuclei, stability to heavy particle emission is the only known information. However, even this information is important because the particle stability of nuclei is a sensitive check of theoretical predictions of masses of nuclei.[4,5] Of particular value are the cases where the limits of nuclear stability can be established this way, as was the case recently for ^{14}Be and ^{17}B.[6]

It is clear, however, that more detailed information on ground and excited states are needed as knowledge progresses on these new nuclear species. Some experiments have already been reported on half-lives[7,2] and mass measurements.[8,9] The spectroscopic information on these short-lived nuclei has been rapidly progressing[10] and recent work[11] shows that it may possibly be extended in the future up to the limits of stability. Particularly important, however, are the measurements of ground state masses of nuclei.

Three different methods have been used to measure masses of exotic nuclei. Nuclear reaction Q values were used to measure the mass of ^{8}He (Ref. 12) at the same time as its decay was studied.[13] Similar Q-value techniques have been applied since to ^{25}Ne,[14] ^{14}B,[15] and ^{26}Na.[16,17] More complex transfer reactions on heavy targets have extended these measurements to nuclei even further from the stability line such as ^{22}O.[8] Also, γ coincident β end-point energies have been used to determine the masses of nuclei with $T_z = \frac{5}{2}$ between ^{23}F and ^{35}P.[10,18-23] Recently it was shown that a single stage mass spectrometer of moderate resolving power, used on-line with an accelerator, could be used to measure masses of short-lived isotopes.[9] These first measurements of $^{27-30}$Na were still of moderate accuracy (200 to 500 keV) but extended to a distance from the stability line ($\Delta T_z = \frac{7}{2}$) that was practically inaccessible to other techniques. In the present paper we wish to report on an extension of these measurements to other nuclei (notably ^{11}Li) and on a substantial improvement in precision, bringing this technique to better than 100 keV accuracy in cases not limited by statistics. The implications of the measurements will also be discussed more fully than had been possible in Ref. 9. The present series of measurements will be referred to as run II. The previous measurements, run I, have been reanalyzed and included in the present paper. Thus, this work supersedes Ref. 9 and the preliminary values from run II previously presented.[24]

II. EXPERIMENTAL

A. Principle of the experiment

The short-lived nuclei of interest are produced in reactions of 24 GeV protons from the CERN proton synchrotron incident on uranium or iridium targets. In the on-line mass spectrometer,[25] a special, heated, target assembly acts as a surface-ionization ion source for a single-stage magnetic spectrometer. The ions passing through the exit of the spectrometer are refocused by a pair of electrostatic quadrupole lenses onto an electron multiplier located in a well-shielded area and able

to detect single ions. In principle, one determines the ratio of two masses, one of which is known and serves as reference mass. In this work, the reference mass was always a lighter isotope from the same element. In order to measure this ratio of two masses, one measures accurately the ratio of the accelerating potentials that cause the ions of the two masses to follow exactly the same trajectory between the entrance and exit slits of the spectrometer.

The on-line mass spectrometric technique[25,26] and its first application to mass measurements[9] have already been described. A more detailed description of the experimental apparatus can be found elsewhere.[27,28] Our description, therefore, will restate briefly only the features which are essential in following the discussion and will put particular emphasis on the new developments which have resulted in obtaining extended and improved results.

B. Target-ion source

The essence of the technique lies in the capture of energetic recoils from the nuclear reaction in heated graphite foils from which alkali elements diffuse very rapidly and can be subsequently ionized on a hot metallic surface.[25] A high degree of chemical selectivity is thus achieved in times which are compatible with even the shortest β half-lives. All the known particle-stable sodium isotopes can be produced by the reaction of high energy protons with uranium.[2] The target was thus made of an assembly of about 100 foils of graphite (70 μm thick) on which a layer of uranium 5 to 10 mg/cm^2 thick had been evaporated. The assembly was wrapped in a 25 μm thick rhenium envelope heated by a dc current (~60 A, 4–5 V) to a temperature in excess of 1600°C [Fig. 1(a)].

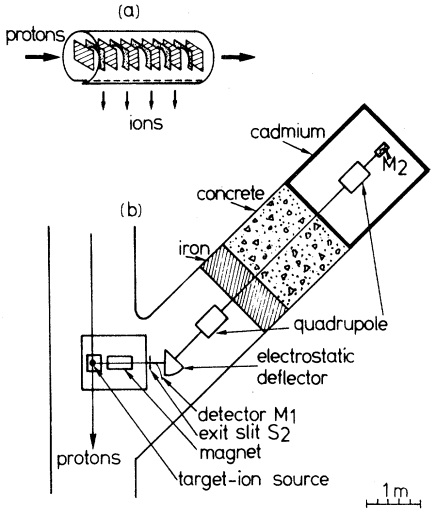

FIG. 1. (a) The target-ion source made of an array of foils wrapped in a rhenium envelope. (b) Setup of the mass spectrometer in the fast extracted beam of 24 GeV protons produced by the CERN synchrotron. The mass spectrometer magnet bends in the vertical plane.

Iridium, rather than uranium, was used as a target to produce ^{11}Li. This (as has been observed earlier[7,26]) is necessary because the effective work function of the ionizing surface is decreased in the presence of uranium. As lithium has a higher ionization potential than sodium, its efficiency of ionization is thus decreased by a factor of 10 while that of sodium is not notably changed. The target then consisted of an array of 100 foils of graphite 70 μm thick and 50 foils of iridium 50 μm thick (100 mg/cm^2), separated by spacers. The total target thicknesses were thus ~1 g/cm^2 of uranium and ~5 g/cm^2 of iridium.

The experiment was placed in the fast extracted beam of the CERN proton synchrotron [Fig. 1(b)]. The full intensity of the accelerator (around 1.5 $\times 10^{12}$ protons) was delivered to our target one burst out of every five (i.e., every 10 s) in a time lasting only 2 μs. The complex pulsed proton beam transport system[29] resulted in a focus of about 2 mm diam, smaller than the dimensions of the target (8 mm diam). The exact position and focus of the proton beam in some runs was found important to the production of short-lived nuclei.

C. The spectrometer

The target-ion source was kept at a positive potential of about 10 kV dc and the ion beam was focused on a defining slit S_1 at ground potential by a system consisting of two intermediate electrodes. The width of slit S_1 could be externally controlled by a micrometer between 0.1 and 2.0 mm. This slit acted as an object for a 90° magnetic sector with a weakly inhomogeneous ($n = 0.23$) field of mean radius 35 cm. In order to maximize the production rates by high energy protons, the target-ion source could be up to 45 mm long, only limited by optical considerations. The inhomogeneous field acted as a weak lens and the size of the beam in the direction of the magnetic field was 15 mm at the place of radial focus. The magnet gap was 50 mm at the mean radius.

In order to achieve the expected resolving power ($M/\Delta M = 650$ at 10% of the peak height) and maintain the best possible transmission, it was necessary to correct the aberrations of the magnet with a point by point shimming procedure that is described in detail elsewhere .[27,28] Figure 2 shows the improvement in resolution that was obtained by the shimming procedure. As will be discussed

in a later section, it is worth noting that even though the precision in the mass measurement was better with the shimmed machine, it was concluded that no systematic error had been caused by the distortion of the peak shape. This is understandable if an objective criterion (mean, median) is used to define the centroid of a peak and if the peak shape does not depend on mass. This later assumption is supported by the over-all precision shown by our calibration procedure. The fact that one compares isotopes of the same element produced and ionized under the same conditions is certainly very favorable in this context. A particular problem arose, however, because the cross sections differed by a factor of as much as 5 orders of magnitude from ^{24}Na to ^{33}Na. In the case of Li, with as few as a hundred ^{11}Li nuclei produced each proton burst, care had to be exercised to avoid distortion of the peak shape caused by dead-time effects in the detector and electronics when as many as 50 000 counts/ms of ^{7}Li were collected on the detector.

D. Background requirements and beam transport system

The ions passing the exit slit of the spectrometer were detected by an electron multiplier. Earlier experiments[2] had shown that the radiation background caused by the intense burst of protons interacting with our target was the limiting factor in detecting rare isotopes. The thermalization and capture of energetic neutrons caused a background tail that extended many milliseconds after the passage of the beam (Fig. 3). The background problem was solved by locating the electron multiplier behind a wall of 60 cm of iron and 1.6 m of concrete. A thin layer of cadmium (0.5 mm thick) served to insure that the thermal neutrons behind the shielding wall were captured quickly, thus suppressing the exponential decay.[30] Figure 4 shows an example of how ^{11}Li stood out clearly above the background.

Because of the shielding requirements, the ions passing through slit S_2 had to be transported through an evacuated pipe in the shielding wall and refocused on the detector. This was done by a system of two symmetric triplets of electrostatic quadrupole lenses. The position and dimensions of the final image after the transport system was studied by displacing the detector M_2 with a 0.1 mm slit, in the two directions r and Z. This procedure will be described in detail elsewhere.[27,28] For typical conditions the beam dimensions were about 4 ×3 mm^2. This was smaller than the active surface of the electron multiplier and was in reasonable agreement with calculations[28] which showed the beam transport system capable of accepting all rays passing slit S_2. During the experiment a rough check of the efficiency of the transport system could be done by comparing count rates on detectors M_1 and M_2 at each end of the transport line (see Fig. 1). One will thus assume that the exit slit of the spectrometer is S_2

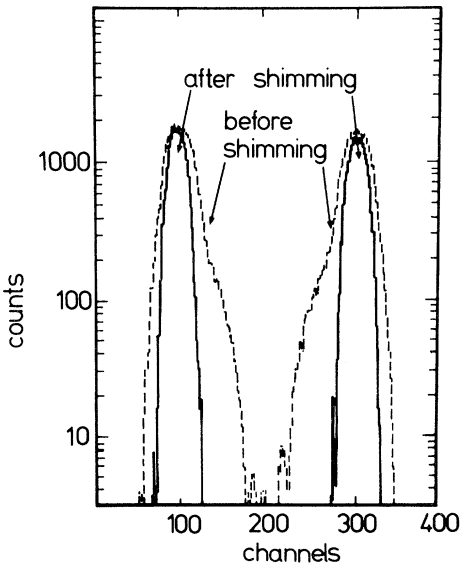

FIG. 2. Improvement of the resolving power of the mass spectrometer, and of the symmetry of the peak shape introduced by the shimming. With the high voltage of 10 kV and 0.4 V per channel, the measured resolving power, full width, at 10% of maximum, is 350 before shimming (run I) and 650 after shimming (run II).

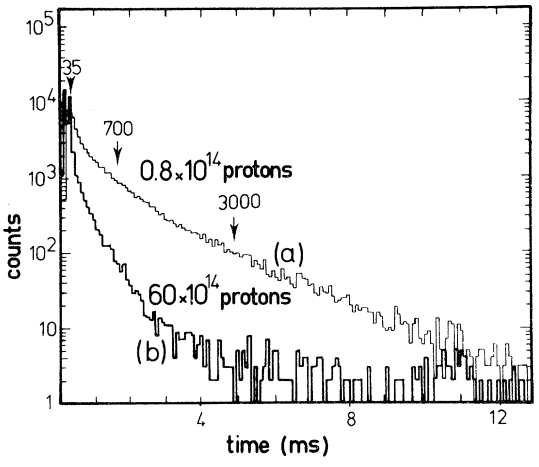

FIG. 3. Measurement of the background after the proton burst which occurs at time 0: (a) Near the mass spectrometer (detector M_1); (b) In the counting room (detector M_2). The background suppression is indicated at three different times by the numbers above the arrows.

only. The potential applied to the transport lenses to insure focusing was maintained proportional to the main accelerating voltage when it was changed to perform the mass measurements, as will be discussed in a later section.

E. Mass measurement procedure

We make use of the well-known theorem[31] that if two ions of masses M_A and M_B are accelerated under potentials V_A and V_B, and if they follow the same trajectory (between slits S_1 and S_2), the following relation holds:

$$\frac{M_A}{M_B} = \frac{V_B}{V_A} . \tag{1}$$

In order to determine exactly the potentials that will match the trajectories, a periodic, calibrated, triangular modulation (linearity better than 1%) is added to a well-stabilized dc power supply in order to sweep the ion beam back and forth across slit S_2. A peak is then recorded with a multiscaler synchronized with the modulation. As is illustrated in Fig. 5, the position of the center of gravity of this peak (i.e., the phase with respect to the modulation) gives a measure of the voltage increment v_A at the time when the ion beam passes the slit. This is then added to the dc component U of the regulated high voltage supply.

On alternate accelerator pulses, data were recorded on two masses by switching two physically distinct dc power supplies by a system of relays and accumulating the corresponding counts in different sections of the multiscaler memory. The system was later modified to measure three masses in succession. The power supplies were stabilized to 10^{-5} and the 6 to 10 kV voltages were measured through a divider bridge by an accurate six-digit digital voltmeter (DVM). Each one of the 100 resistors of the divider bridge had a temperature variation of 2×10^{-6} per degree centigrade, and the whole bridge was immersed in oil.

A measurement would consist of a number of such alternate mass sweeps in order to have adequate statistics for both masses. This could last from 10 to 30 min (or longer for low yield isotopes) and during this time, the DVM readings—interfaced to a PDP-15 computer—were averaged out (see Sec. III A). The stability of the dc voltages as measured during a run came to about 0.1 V (or 10^{-5}), and did not seem to be the limiting factor in the precision of the measurements as discussed in a later section. At the end of a run, the data were transferred from the multiscaler to the computer and could be stored on magnetic tape and processed while data for the next run were accumulated. The data processing involves mainly subtraction of backgrounds and calculation of the

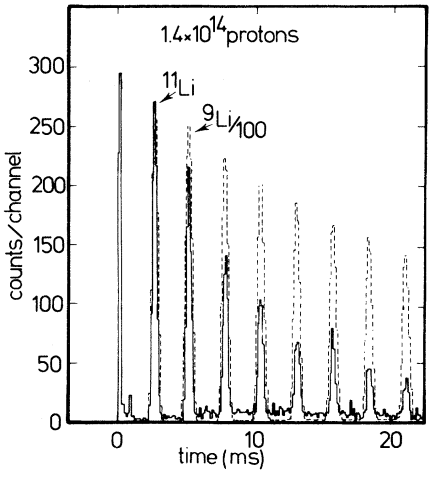

FIG. 4. Spectra of ^{11}Li and ^{9}Li: Four pairs of peaks are recorded following the proton burst which occurs at time 0. It may be seen that ^{11}Li stands very clearly over the background and decays very much faster than ^{9}Li, due to its short half-life of 8.5 ms.

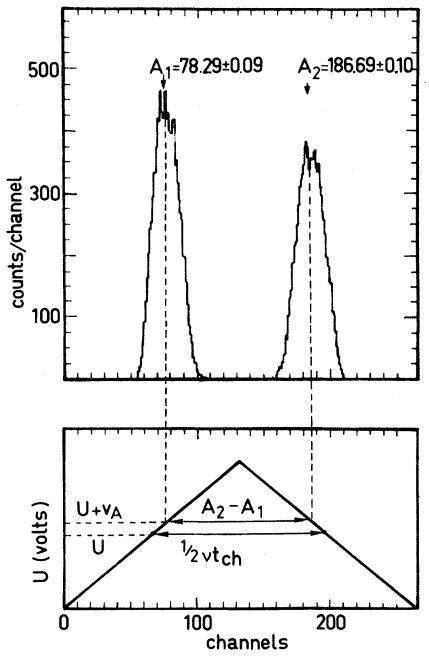

FIG. 5. Time spectrum (upper part of the figure) of the ion current recorded in a mode synchronized with the modulated accelerating voltage (lower part). U is the average dc voltage (6–10 kV). The triangular modulation amplitude was typically 50 V peak to peak and had a frequency of 40–250 cycles/s. The vertical dashed lines indicate the centers of gravity of the mass peaks. The quantity $(2\nu t_{ch})^{-1}$ is one-half the period of modulation. See text for further explanations.

centroids of the peaks, as will be explained later (Secs. III C and III D).

The amplitude of the triangular modulation was adjusted in order to cover completely the peak width and give enough channels for background subtraction on either side. This came to about 50 V peak-to-peak (0.5% of the total voltage) in typical conditions.

F. Determination of systematic errors

In order to determine the systematic errors, formula (1) was modified and a parameter δ introduced so that:

$$\frac{M_A}{M_B} = \frac{V_B + \delta}{V_A + \delta}, \tag{2}$$

with δ being measured by using pairs of known masses produced under the same experimental conditions. During run I, the values of δ were found to be many volts and could not be neglected. It was conjectured that the parameter δ reflected the presence of many causes of systematic errors which could not be eliminated. The most bothersome point was not the absolute value of δ but rather its time variation. The procedure which had been adopted was thus to calibrate each "mass measurement" by δ measurements done immediately before and after, and differing by the same mass number jump. While this procedure gave good results, a further refinement was introduced during run II whereby three masses (M_A, M_B, and M_C) could be recorded in succession. If M_B and M_C are known masses, δ is continuously measured and one is freed of its time variation in determining the unknown M_A. This is at the obvious expense of some complication in the hardware (three power supplies, etc.), routing logic, and data processing. In order to test the value of this concept one had first to apply it to three known masses. One can then define three quantities, δ_{AB}, δ_{AC}, and δ_{BC}, from trivial modification of Eq. (2).

The results were disappointing because quantities such as $\Delta = \delta_{BC} - \delta_{AC}$ were not only different from zero but also varied with time. It thus seemed necessary to calibrate (as was done in run I[9]) each mass measurement by a succession of δ and Δ measurements before and after. The only improvement so far, over run I, was that Δ showed dispersions about three times less than δ (Table I). After a long series of measurements discussed in a later section the measuring bridge referred to as B was replaced by a new one referred to as B′. All the measurements done subsequently showed values of δ smaller than 1 V, with Δ values compatible with zero (see Table I). It was later discovered that the value of one of the resistors in bridge B varied according to the applied voltage. However, the measurements done with both bridges are discussed in the next sections and are shown to be compatible. Since the three known sodium isotopes used for the Δ measurements were 22, 25, and 26, the assumption of $\Delta = 0$ when B′ was used gives, as a by-product, a new high precision check of the known,[16,17,19] mass of ^{26}Na, as discussed in a later section.

G. Variation of δ with time after the proton burst

The interaction of the beam of protons with our target caused a slight, but noticeable, displacement of the peak position. This indicates that the value of the dc potential of the target changed. The δ values obtained varied with time after the beam burst. The reason for this variation in the target potential is not fully understood but is thought to be due to the release of secondary electrons.

The magnitude of this additional δ can be of the order of 2 V and is found to damp out some 10 ms after the beam burst. In most of the mass measurements, one introduced an adequate delay after the beam burst before starting data accumulation. This is not possible in the case of the shortest lived isotopes like ^{11}Li ($T_{1/2} = 8.5$ ms). It was

TABLE I. Typical δ and Δ values during the two runs of mass measurements. The first pair of peaks after the proton beam had typical values about 2 V higher and a worse dispersion.

Run	Number of masses in the cycle	Bridge	ΔM	δ (V) Value	δ (V) Dispersion	Δ (V) Value	Δ (V) Dispersion
I	2	B	1	13 to 26	0.6 to 1.9		
I	2	B	2	~13	0.6 to 1.9		
I	2	B	3	3 to 8	0.6 to 1.9		
I	2	B	4	5 to 10	0.6 to 1.9		
II	2	B	any	15 to 25	1.5 to 3		
II	3	B	any	(25 to 35)		−1 to +1	0.5 to 1
II	2 or 3	B′	any	~−0.5	0.3	0.0	0.2

found necessary in this case to record the entire sequence of peaks as a function of time after the beam burst (see Fig. 4). The improved procedure complicated somewhat the data analysis but did not cause any loss in statistics since the data corresponding to each pair of peaks with their own δ value were combined later on as discussed in the next section.

III. DATA PROCESSING AND ERROR ESTIMATION

As explained before, the basic formula is Eq. (2), in which V is obtained by adding an increment v, depending on the position of the peak, to the measured dc voltage U.

A. Measurement of the dc voltage U

U, which is between 6 and 10 kV, is divided by 10^4 by the special divider bridge (B or B′) (see Sec. IIE) and then measured by the DVM. Each measurement of U lasts 1 s, starting from the beginning of the mass measurement, and is then automatically recorded by the computer. The computer identifies the voltage (A, B, or C), and calculates a running average $\overline{U}_N$. The dispersion of the N measurements is also estimated (see Appendix A). However, if this dispersion is due only to fluctuations of the voltage applied to the ions, it does not have to be taken into account in the error estimation. This is because it is already included in the statistical error on the position of the peak, since its only effect is to broaden the peak which then decreases the accuracy of the calculation of the centroid.

B. Calculation of the increment v

The position of a peak may be characterized by its center of gravity (mean) or its median. If there exists a nonzero δ, its value may be slightly changed according to the method chosen, but the final mass must be the same. This result was checked by performing all calculations using both the mean and the median (see Appendix B).

For a given mass A, the centroids of the two peaks corresponding to the ion beam sweeping back and forth across the slit are called A_1 and A_2 (Fig. 5). The voltage v_A is calculated by comparing the distance between the peaks $(A_2 - A_1)$ to the distance corresponding to phase zero, which is equal to one-half of the period of the triangular modulation:

$$v_A = \tfrac{1}{2} V_{\mathrm{ch}} \left[\frac{1}{2\nu t_{\mathrm{ch}}} - (A_2 - A_1) \right], \tag{3}$$

where ν is the frequency of the triangular modulation (40–250 cycles/s) which is measured to better than 1%, t_{ch} is the time per channel, and V_{ch} is the number of volts per channel. In order to measure V_{ch}, we recorded the same mass with different applied voltages U and plotted U versus $A_2 - A_1$. Then V_{ch} is twice the slope calculated by a least squares fit. With the resolving power of 650 at 10% of the peak and 250 channels, V_{ch} was typically about 0.3 V per channel. The accuracy of this measurement was generally 1%, while the values of v were around 1 V.

C. Determination of the systematic corrections

Measuring two known masses M_A and M_B, δ was easily calculated from Eq. (2). When there were three masses, M_A, M_B, and M_C, Δ was defined as

$$\Delta = \delta_{BC} - \delta_{AC} . \tag{4}$$

From the statistical uncertainty of the centroids, it is possible to calculate the error due only to these statistics for V_{ch}, v, and δ or Δ. Unfortunately, with the bridge B, it appeared that during run I, the values of δ were dependent on the mass difference $M_A - M_B$, while during run II, δ and Δ were not noticeably dependent on the differences $M_B - M_C$ or $M_A - M_C$. However, with three masses, they depended very much on the sequence: ABC, ACB, or $CBCA$. In all cases δ or Δ were fluctuating very much more with time than predicted by statistical considerations. To take into account all these difficulties, we recorded series of spectra with the same mass jump during run I, or the same sequence during run II.

For such a series of n spectra, first we calculated the values δ_i or Δ_i corresponding to each spectrum. Then we calculated their mean values $\overline{\delta}$ or $\overline{\Delta}$ and used their dispersion as an estimation of their uncertainty. The results obtained in the different cases are summarized in Table I. As indicated before, we finally discovered that these high values of δ and their dependence on mass jump or sequence were mainly due to a faulty resistor of the bridge B. With the bridge B′, Table I shows that we obtained very small values of δ and zero values for Δ.

In the cases where the entire sequence of peaks is recorded as a function of time after the beam burst, the procedure is more sophisticated, as the first pair of peaks must be processed separately because of the influence of the beam on the high voltages, while the subsequent pairs may be added together. Then the different spectra were combined as before and provided two values of $\overline{\delta}$ or $\overline{\Delta}$: $\overline{\delta}_1$ or $\overline{\Delta}_1$ for the first pair of peaks and $\overline{\delta}_2$ or $\overline{\Delta}_2$ for all the others. Their dispersions are σ_1 and σ_2. However, as there is only one mea-

surement of U for all pairs of peaks, σ_1 and σ_2 are not independent; σ_2 is due to the fluctuation of the divider bridge while σ_1 reflects the same fluctuations plus the fluctuations of the change of high voltage produced by the beam burst. So we can calculate these two effects instead of σ_1 and σ_2 and get for the divider bridge fluctuations

$$\sigma_{\text{bridge}}{}^2 = \sigma_2{}^2 , \tag{5}$$

and for the beam burst fluctuations

$$\sigma_{\text{beam}}{}^2 = \sigma_1{}^2 - \sigma_2{}^2 . \tag{6}$$

D. Calculation of the masses and their errors for each spectrum

In the normal situation when all pairs of peaks are already added together, the unknown mass M_A was calculated by use of Eq. (2) in which δ is taken equal to $\bar{\delta}$ for the two mass case, or to $\delta_{BC} - \bar{\Delta}$ for the three mass case.

The error on M_A was calculated taking into account the uncertainty of $\bar{\delta}$ or $\bar{\Delta}$ (estimated by their dispersions) and the statistical errors during the measurement of M_A, i.e.:

$$\sigma^2(M_A) = M_A{}^2 \sigma_{\text{stat}}{}^2 + (\Delta M / V_A)^2 \sigma^2(\bar{\delta} \text{ or } \bar{\Delta}), \tag{7}$$

where $\Delta M = M_A - M_B$ or $M_A - M_C$ according to the cycle and with

$$\sigma_{\text{stat}}{}^2 = \frac{V_{\text{ch}}{}^2}{2}\left[\frac{\sigma^2(A)}{V_A{}^2} + \frac{\sigma^2(B \text{ or } C)}{V_{B \text{ or } C}{}^2}\right], \tag{8}$$

where $\sigma(A)$, $\sigma(B)$, or $\sigma(C)$ are the statistical errors on the determination of the centroids of the peaks of A, B, or C.

In the more sophisticated case where the sequence of peaks is recorded as a function of time, two values of M_A are calculated: M_{A1} for the first pair of peaks and M_{A2} for the others. Their errors are the statistical ones, but for M_{A1}, $\sigma_{\text{beam}}{}^2$ was also taken into account:

$$\begin{aligned} \sigma^2(M_{A1}) &= M_A{}^2 \sigma_{\text{stat}}{}^2 + (\Delta M / V_A)^2 \sigma_{\text{beam}}{}^2 , \\ \sigma^2(M_{A_2}) &= M_A{}^2 \sigma_{\text{stat}}{}^2 . \end{aligned} \tag{9}$$

Then M_A is the weighted mean value of M_{A1} and

TABLE II. Experimental results for the mass excess of ^{11}Li. All of the data are from run II and were collected as a function of time after the beam burst.

Masses used δ or Δ	Masses used Mass	$(M-A)$ experimental (keV)	Bridge
7-9	9-11	39 983 ± 462	B
7-9	9-11	40 340 ± 525	B
8-9	9-11	41 070 ± 161	B
8-9	9-11	40 814 ± 168	B
6-9	8-11	41 238 ± 580	B
6-9	9-11	41 676 ± 357	B
7-9	9-11	40 959 ± 422	B
7-9	9-11	40 818 ± 415	B
8-9	9-11	41 296 ± 542	B
(a)	8-9-11	41 002 ± 163	B′
(a)	8-9-11	40 891 ± 158	B′
(a)	7-9-11	40 593 ± 477	B′

[a] Δ is an averaged value between 6-7-9, 6-8-9, and 7-8-9 data, compatible with zero.

TABLE III. Experimental results for the mass excess of ^{26}Na (keV). All measurements were done during run II with the bridge B′. In the two-mass measurements 22-25 and 22-26 were used, respectively, for calibration and mass measurement. In the three-mass measurements, masses 22-25-26 were used and it was assumed that Δ = 0. In all cases data were collected as a function of time and only the second, third, and fourth pair of peaks have been taken into account.

Two-mass measurements	Three-mass measurements
−6792 ± 190	−6733 ± 110
−6790 ± 190	−6960 ± 100
−6987 ± 190	−6982 ± 110
−6947 ± 190	−7138 ± 115
−6900 ± 190	−6842 ± 115
−6948 ± 190	−6751 ± 190
−6854 ± 140	−7053 ± 195
−6972 ± 140	−6979 ± 213
−6946 ± 140	−6852 ± 110
−7006 ± 140	−6836 ± 110
−7102 ± 140	−6680 ± 95
−6903 + 140	−6816 ± 95
	−6935 ± 100
	−6984 ± 100

TABLE IV. Experimental results for the mass excess of ^{27}Na.

Masses used δ or Δ	Masses used Mass	$(M-A)$ experimental (keV)	Run	Bridge
(a)	26-27	−5253 ± 255	I	B
(a)	26-27	−5870 ± 270	I	B
25-26	26-27	−5846 ± 210	I	B
25-26	26-27	−5547 ± 210	I	B
22-24	25-27	−5741 ± 155	I	B
22-24	25-27	−5590 ± 150	I	B
25-26	26-27	−5923 ± 255	II	B
25-26	26-27	−5602 ± 250	II	B
(Δ = 0)	22-26-27	−5578 ± 195 [b]	II	B′
(Δ = 0)	22-26-27	−5433 ± 195 [b]	II	B′
(Δ = 0)	22-26-27	−5513 ± 190 [b]	II	B′

[a] δ is an averaged value from 24-25 and 25-26 data.
[b] Data collected as a function of time after the beam burst (see text).

M_{A2}. The contribution of $\sigma_{\text{bridge}}{}^2$ is added to the error deduced from the errors on M_{A1} and M_{A2} in order to get the final error on M_A:

$$\sigma^2(M_A)=\frac{1}{1/\sigma^2(M_{A1})+1/\sigma^2(M_{A2})}+\left(\frac{\Delta M}{V_A}\right)^2\sigma_{\text{bridge}}{}^2 .$$

IV. RESULTS

All the individual results are shown in Tables II to IX. This method measures the masses of singly ionized atoms, but the results are presented in terms of the mass excesses $(M-A)$ of the neutral atoms. In Table X the final values for each mass are the weighted means of all individual results. The reference mass values were taken from Wapstra and Gove (I).[32] When the reference mass was not accurately known (e.g., mass 29 measured with a 28-29 cycle), an intermediate weighted mean value was calculated and the uncertainty in the reference mass then folded in. The error on the adopted value is the standard error.

TABLE V. Experimental results for the mass excess of ^{28}Na. The asterisks show the values deviating more than 2.5 σ.

Masses used δ or Δ	Mass	$(M-A)$ experimental (keV)	Run	Bridge
22-25	25-28	−1754 ± 300	I	B
22-25	25-28	−1702 ± 300	I	B
22-25	25-28	−808 ± 500	I	B
22-25	25-28	−1489 ± 315	I	B
22-25	25-28	−1197 ± 375	I	B
22-25	25-28	−309 ± 370	I	B
25-26	27-28	−1858 ± 240 [a]*	I	B
25-26	27-28	−1984 ± 250 [a]*	I	B
22-24	26-28	−1094 ± 360	I	B
22-25	25-28	−152 ± 560	I	B
22-25	25-28	−1853 ± 545	I	B
22-25	25-28	−632 ± 535	I	B
22-25	25-28	−750 ± 570	I	B
22-25-26	25-26-28	−1357 ± 335	II	B
22-25-26	25-26-28	−820 ± 380	II	B
22-24	26-28	−1017 ± 990	II	B
(b)	25-26-28	−346 ± 190 [a]*	II	B
(b)	22-25-28	−1746 ± 205 [a]*	II	B
(b)	25-26-28	−712 ± 195 [a]	II	B
22-25-26	22-26-28	−434 ± 700	II	B
22-25-26	22-25-28	−861 ± 600	II	B
22-25-26	22-25-28	−1327 ± 595	II	B
(Δ = 0)	22-26-28	−1056 ± 245 [c]	II	B′
(Δ = 0)	22-26-28	−1127 ± 240 [c]	II	B′
(Δ = 0)	22-26-28	−998 ± 240 [c]	II	B′

[a] Rejected value (see text).
[b] Δ is an averaged value between 22-25-26 and 21-22-26 data.
[c] Data collected as a function of time after the beam burst (see text).

TABLE VI. Experimental results for the mass excess of ^{29}Na.

Masses used δ or Δ	Mass	$(M-A)$ experimental (keV)	Run	Bridge
22-25	26-29	3133 ± 420	I	B
22-25	26-29	2876 ± 480	I	B
22-25	26-29	2550 ± 470	I	B
22-25	26-29	3125 ± 480	I	B
22-26	25-29	2691 ± 720	I	B
22-26	25-29	2799 ± 760	I	B
22-26	25-29	2843 ± 740	I	B
25-26	28-29	2343 ± 350	I	B
25-26	28-29	2590 ± 410	I	B
22-26	25-29	2923 ± 570	I	B
22-25	26-29	3067 ± 630	I	B
22-25	26-29	2686 ± 720	I	B
22-25	26-29	3804 ± 840	II	B
22-26	25-29	4485 ± 1300	II	B
22-25	26-29	4292 ± 980	II	B
22-25-26	22-26-29	1801 ± 770 [a]	II	B
22-25-26	22-26-29	2000 ± 760 [a]	II	B
(Δ = 0)	22-26-29	2384 ± 220 [a]	II	B′
(Δ = 0)	22-26-29	2723 ± 230 [a]	II	B′
(Δ = 0)	22-26-29	2512 ± 220 [a]	II	B′

[a] Data collected as a function of time after the beam burst (see text).

If our estimation of the uncertainties is correct, the experimental values of χ^2 should be within the limits of the χ^2 values predicted by statistics. It appears from Table X that all the values are compatible, except for ^{28}Na. Testing our method on the seven other masses, we get $\chi^2 \sim 73$ for 89 measurements for which the expected value would be

TABLE VII. Experimental results for the mass excess of ^{30}Na.

Masses used δ or Δ	Mass	$(M-A)$ experimental (keV)	Run	Bridge
22-26	26-30	8813 ± 620	I	B
25-26	29-30	9404 ± 910	I	B
25-26	29-30	8474 ± 780	I	B
22-26	26-30	7399 ± 890	I	B
22-26	26-30	9750 ± 1480	II	B
22-25-26	22-25-30	7854 ± 940	II	B
22-25-26	22-26-30	7522 ± 1200 [a]	II	B
22-25-26	22-26-30	6407 ± 1190 [a]	II	B
22-25-26	22-26-30	7507 ± 920 [a]	II	B
(Δ = 0)	22-26-30	8393 ± 450 [a]	II	B′
(Δ = 0)	22-26-30	8799 ± 530 [a]	II	B′
(Δ = 0)	22-26-30	8376 ± 440 [a]	II	B′

[a] Data collected as a function of time after the beam burst (see text).

TABLE VIII. Experimental results for the mass excess of ^{31}Na. Data were collected in run II with bridge B as a function of time after the beam burst.

Masses used δ or Δ	Mass	$(M-A)$ experimental (keV)
22-25-26	22-26-31	9720 ± 1620
22-25-26	22-26-31	11 880 ± 1520
22-25-26	22-26-31	10 390 ± 1060

TABLE IX. Experimental results for the mass excess of ^{32}Na. Data were collected in run II with bridge B as a function of time after the beam burst. Only the first pair of peaks could be used because of the lack of statistics.

Masses used δ or Δ	Mass	$(M-A)$ experimental (keV)
22-25-26	22-26-32	17 940 ± 2000
22-25-26	22-26-32	14 960 ± 2150
22-25-26	22-26-32	20 120 ± 2440
22-25-26	22-26-32	11 780 ± 2440
22-25-26	22-26-32	19 220 ± 5070

81.5 ± 13. From this, we may conclude that in general our estimation of the uncertainties is correct. Considering now the case of ^{28}Na, we get $\chi^2 = 74$ for 25 measurements, while it is expected to be 23^{+8}_{-6}. The probability of such a deviation ($\sim 6\sigma$) is about 10^{-9}. To check more carefully what happened, we drew a histogram of the number of measurements versus χ_i (Fig. 6). It shows that in 21 cases $|\chi_i| \leq 2$, while in the four others we get $|\chi_i| > 2.5$. These four measurements have an asterisk in Table V and one sees that they come from only two series of measurements, one during run I, and the other during run II. Our conclusion is that something was wrong in these two series (potentials of the triplets not well adjusted, for example) and that we have to reject the five spectra of these series. Fortunately, the mean value of the 20 measurements remaining is very close to the one including all the data: −1140 instead of −1170, and χ^2 is now 23 when the expected value is 18^{+7}_{-6}. Then, for the whole experiment of 109 measurements, we get

$$\chi^2 = 96 \quad \text{(Expected value} = 100 \pm 14\text{)}.$$

This indicates that all the measurements are compatible, whether they were done with two or three mass cycles or with the bridge B or B′.

Our value for ^{26}Na is accurate to 25 keV, which is one part per million. For this isotope two previous values existed in the literature: −6853 ± 30 keV by Ball *et al.*[16] and −6903 ± 20 by Flynn and Garret.[17] Our value agrees with the measurement of Flynn and Garret, confirming, as they suggested, that the value of Ball *et al.* was influenced by an unresolved first excited state at 80 keV. Combining our measurement with that of Flynn and Garret and the β endpoint measurement of Alburger, Goosman, and Davids[19] gives a best value for the mass excess of ^{26}Na equal to −6902 ± 15 keV. One last remark to be noted is that in the case of ^{27}Na, it was necessary to check that there was either no contamination due to natural ^{27}Al, or that it was small enough so that it was possible to subtract it. All spectra in which the contamination was not small were rejected. If we combine our value with that of Alburger, Goosman, and Davids,[19] the best value becomes −5625 ± 55 keV.

TABLE X. Adopted values for the experimental mass excesses of ^{11}Li and $^{26-32}$Na.

Isotope	$M-A$ (keV)	Number of measurements	χ^2 experimental	χ^2 expected
^{11}Li	40 940 ± 80	12	13	10^{+6}_{-4}
^{26}Na	−6901 ± 25	26	21	24^{+8}_{-7}
^{27}Na	−5620 ± 60	11	7	9^{+5}_{-4}
^{28}Na	(−1170 ± 60) [a]	(25)	(74)	(23^{+8}_{-6})
	−1140 ± 80	20	23	18^{+7}_{-6}
^{29}Na	2650 ± 100	20	15	18^{+7}_{-6}
^{30}Na	8370 ± 200	12	9	10^{+6}_{-4}
^{31}Na	10 600 ± 800	3	1.0	$1.4^{+2.5}_{-1.0}$
^{32}Na	16 400 + 1100	5	7.3	$3.4^{+3.5}_{-2.0}$

[a] Original value before the rejection of suspicious measurements.

V. DISCUSSION

A. Mass of ^{11}Li

This mass excess was an interesting puzzle because ^{11}Li was very generally predicted to be unbound before it was identified in 1966 by Poskanzer, Cosper, Hyde, and Cerny.[33] The binding energy of its last pair of neutrons, as measured in this work, is very small: $E_{2n} = 170 \pm 80$ keV. We also measured the branching ratio P_n for delayed neutrons[11] and the half-life[7,11] of ^{11}Li. From all three, we can deduce a probable decay scheme (Fig. 7). ^{11}Be has only one bound excited level at 320 keV. As its ground state is $\frac{1}{2}$+ while the excited level is $\frac{1}{2}$−,[34] ^{11}Li decays towards only one of these two levels with a $\log ft = 5.0$. Because it is very probable that the ground state of ^{11}Li is of negative parity it is shown in Fig. 7 as decaying towards the excited level of ^{11}Be.

Different kinds of estimates of the mass excess of ^{11}Li have been done. For such a light and exotic nucleus, however, the empirical extrapolations based on systematic studies of binding energies or the semiempirical general formulas cannot be very reliable. The transverse relations of Garvey and Kelson cannot provide the mass of ^{11}Li without an estimate of the unknown mass of ^{10}Li. However, one can turn the argument around and, using the measured mass of ^{11}Li, try to predict the masses of ^{10}Li and ^{10}He. One finds that both nuclei must be unbound, in agreement with experiment.[33,35]

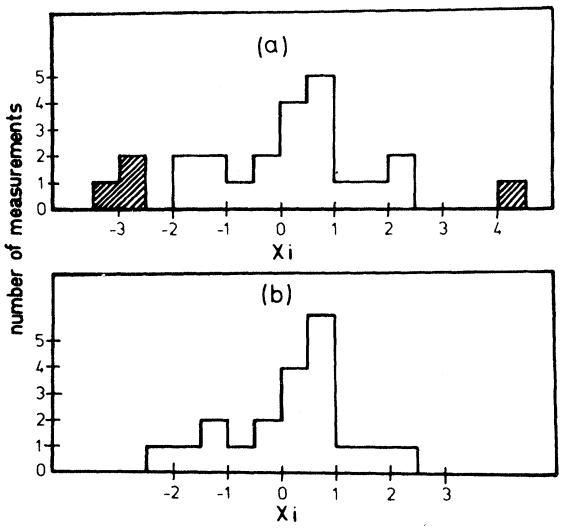

FIG. 6. Histogram of the number of measurements versus χ_i for ^{28}Na: (a) with all 25 measurements, 4 measurements (shaded area) appear with very large value of χ_i; (b) without the suspicious measurements, the remaining measurements show a normal dispersion.

In Table XI we have only reported values calculated in the framework of the shell model: J and T are assumed to be good quantum numbers and the effective interactions are calculated with parameters fitted to known levels in the $1p$ shell. Cohen and Kurath[36] have adjusted parameters for two-body interactions while Goldhammer, Hill, and Nachamkin[37] have also included three- and four-body interactions with a better selection of experimental data. The results of these calculations applied to predictions of ground state binding energies[26] show relatively good agreement, especially with the parameters from Goldhammer.

The available calculated values of $\log ft$ for this decay have also been reported in Table XI: they come from Cohen and Kurath and from a similar calculation done by Hock with L-S coupling according to the method of Boĭarkina.[38] The agreement is very good in this last case and fairly good also with the Cohen and Kurath parameters. By combining the experimental mass excess and the values of $\log ft$ calculated for the decay of ^{11}Li to the computed excited levels of ^{11}Be,[26] it is possible to also deduce the P_n value and half-life of ^{11}Li. These are shown in Table XI to be in reasonable agreement with the experimental data.

B. Sodium masses

The results of the present work, along with other previously known masses of sodium isotopes[32] are plotted in Fig. 8. The curve is asymmetric mainly because it is a cut through the mass surface at constant Z instead of the usually presented cut at constant A. It should be noted that the range of measured isotopes covers N/Z ratios from 0.7 to 1.9 and that the curve extends to more than 25 MeV above the minimum. To our know-

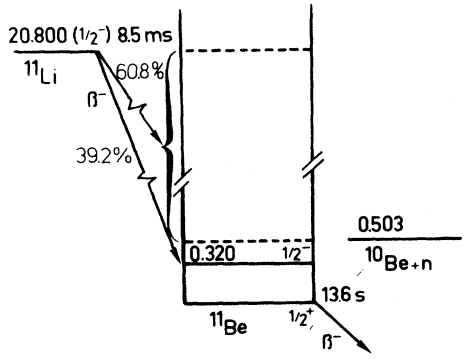

FIG. 7. Decay scheme of ^{11}Li as deduced from the mass measurement described in this work, and from the P_n measurement described in Ref. 11. It is assumed that the ground state of ^{11}Li has negative parity so that it does not decay to the $\frac{1}{2}$+ ground state of ^{11}Be. All energies are in MeV.

ledge, this is the biggest excursion to date away from the bottom of the valley of stability. These results should therefore provide a sensitive test for terms in the mass formulas which would not show up closer to stability.

We have compared our results with four basically different theoretical approaches to the problem of nuclear masses. These are the liquid drop model, a large scale shell model calculation, the Garvey-Kelson method, and a Hartree-Fock calculation. Shown in an expanded scale in Fig. 9 are the differences between the calculations and the experimental mass excesses $(M-A)$.

The Myers and Swiatecki 1965 calculation[39] is based on a liquid drop model with *ad hoc* corrections for shells. The over-all agreement is seen to be fair in Fig. 9. It should be noted, however, that subsequent calculations by the same authors giving an improved over-all fit for heavier masses[40] give poorer results for the sodium masses by several MeV. It is therefore probable that the agreement in 1965 for Na was somewhat fortuitous and that the liquid drop model is inadequate for such light nuclei. One should furthermore note that the various calculations based on the Strutinsky method for shell corrections to the liquid drop, such as those of Seeger and Howard,[41] have not to date been applied to the light nuclei which we have studied, despite their success for heavier masses.

A recent approach to the study of s-d shell nuclei is the untruncated shell model calculation by Cole, Watt, and Whitehead.[42] This calculation uses effective two-body interactions fitted by Kuo[43] or by Preedom and Wildenthal[44] on low T levels of nuclei near the stability line. The results, reported on Fig. 9, seem in good agreement with our experimental values up to ^{29}Na, but the trend indicates a large divergence for ^{30}Na. It is difficult to draw definite conclusion in the absence of calculations for masses 31 and 32. We could remark, however, that they suggest that their results are inaccurate for masses $A \geq 30$. As the interactions are fitted only on low T levels, the present measurements on high T_z states might therefore provide a constraint on the form of the effective nucleon-nucleon interaction to be used in these extensive shell model calculations.

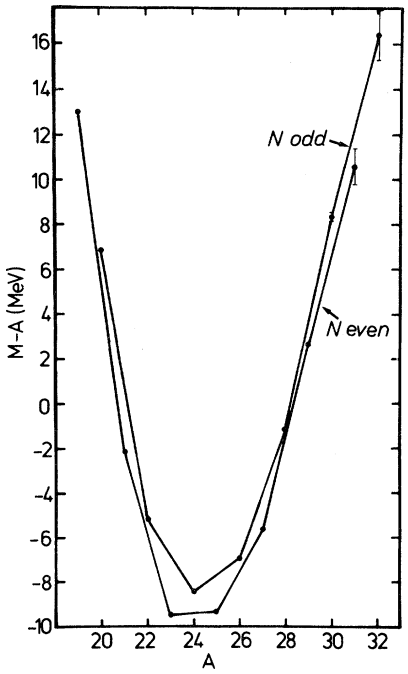

FIG. 8. Experimental mass excesses for all known sodium isotopes.

The Garvey-Kelson method[4] is based on local relationships between neighboring masses which should be satisfied in the framework of a simple independent-particle model of the nucleus. Single particle aspects are very naturally taken into account and this has proven remarkably successful when applied to light nuclei where these aspects tend to be relatively more important than liquid drop aspects[6]. This calculation has been performed for light masses ($Z \leq 17$), using two different sets of parameters adjusted by least squares fit procedures. The first set (GK I) has been fitted on experimental masses with $T_z \leq 2$.[5] Figure 9 shows that the calculated masses diverge monotonically from $A = 26$ to 30, while for $A = 31$ and

TABLE XI. Comparison of experimental and calculated values of the mass excess and of the binding energy of the last pair of neutrons of ^{11}Li. The predicted P_n and half-life are obtained by combining the calculated logft and the experimental mass excess.

	Mass excess (keV)	E_{2n} (keV)	logft	P_n (%)	$T_{1/2}$ (ms)
Experimental	40 940 ± 80	+170 ± 80	5.0	60.8	8.5 ± 0.2
Cohen-Kurath	42 000	−900	4.65	48	5.3
Goldhammer	40 900	+200			
Hock			4.93	79	5.3

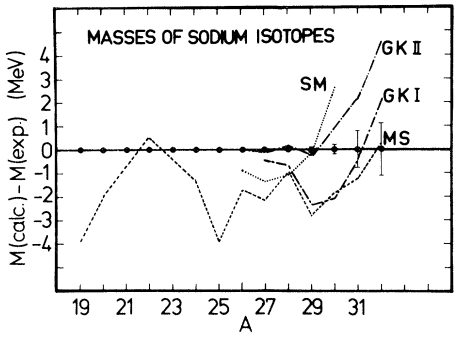

FIG. 9. Differences between the calculated and experimental mass excesses. The different calculations are: MS, liquid drop model from Myers and Swiatecki (Ref. 39); SM, shell model from Cole, Watt, and Whitehead (Ref. 42); GK, Garvey *et al.* relations I (Ref. 5) and II (Ref. 45). In the upper part of the plane the calculated values are less bound than the experimental values.

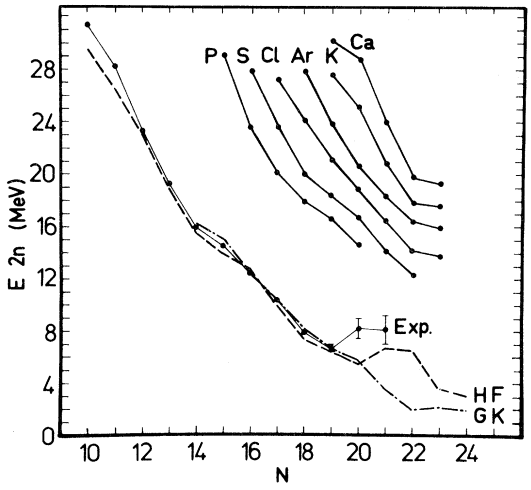

FIG. 10. Values of the separation energies of the last pair of neutrons. The experimental values for the sodium isotopes (solid line) exhibit a hump at $N=20$ and 21. This is shown by none of the experimental values for other elements, nor by the calculations shown in Fig. 9 such as the Garvey *et al.* (GK) relations II(Ref. 45). The only theoretical calculation reproducing this feature is the Hartree-Fock (HF) calculation (Ref. 46) described in the text.

32 an abrupt reversal of this trend appears. With the second set of parameters (GK II), which includes also masses with $T_z=\frac{5}{2}$ and our experimental sodium masses with $A\leq 30$,[45] the diverging trend is corrected and the fit is very good until $A=30$. However, the abrupt change observed for $A=31$ and 32 becomes even more apparent. As the Garvey-Kelson approach retains only the smoothly varying features of the nuclear energy surface, these deviations from the model could indicate the sudden onset of a change of nuclear shape.

Support for this possibility can be obtained theoretically, by Hartree-Fock calculations to be discussed shortly, and experimentally, by plotting the measured two-neutron separation energies versus neutron number (Fig. 10). This plot reveals a rather striking feature. Our data for ^{31}Na and ^{32}Na indicate a hump at $N=20$ and 21 which does not appear in the experimental values for other elements closer to stability. It is worth reminding the reader that similar E_{2n} graphs presented by Wapstra and Gove[32] (IV) show that for prominent shells (not for $N=20$) the curves are smooth right up to the filling of the shell, and then drop suddenly when the next shell begins to fill. It is well known that in regions where a rapid phase transition occurs (as in the region $N=88$ to 92) such curves flatten out or even rise somewhat. Then the behavior of the experimental data for the sodium isotopes at $N=20$ is inconsistent with the classic shell closure effect, and more reminiscent of the behavior one observes when entering a region of sudden deformation.

Interesting light on this question is shed by recent Hartree-Fock calculations[46] since such calculations readily give nuclear radii and deformations. For Na nuclei in the middle of the shell and close to stability a rather deformed prolate shape ($Q_p=48$ fm^2 for ^{23}Na) is predicted. For nuclei further away from stability, as $N=20$ is approached, the Hartree-Fock calculations of Ref. 46 yield two possible prolate solutions corresponding to two minima of comparable energy. Whereas the first minimum corresponds to a more spherical shape, a rather large deformation (Q_p ~ 56 fm^2 for ^{31}Na and ^{32}Na) is associated with the second solution. That solution is definitely the stablest when special care is taken to add the rotation energy. It is seen in Fig. 10 that it reproduces well the upward trend of the two-neutron separation energy around $N=20$.[47] The reason why the onset of the deformation comes one mass number higher than in the experiment will be discussed in Ref. 46. The results of these Hartree-Fock calculations are quite unusual in that they predict a region of strong deformation at a neutron number of 20, which, in the ^{40}Ca region, corresponds to a well-known spherical closed shell. The question of whether or not this is a new region of deformation must, however, await further experimental and theoretical evidence.

ACKNOWLEDGMENTS

It is a pleasure to acknowledge the excellent contributions of R. Fergeau, M. Jacotin, and J. F. Kepinski who built the mass spectrometer and related equipment and assisted during the run at

CERN. We thank G. Le Scornet for preparing the targets and assistance in computer programming. We are grateful to Alan Ball and all the members of the CERN heavy liquid bubble chamber group whose help was essential in installing the experiment and maintaining the complex proton beam transport. We are indebted to X. Campi, H. Flocard, A. Kerman, and S. Koonin for valuable discussions and for making the results of their calculations available to us before publication.

APPENDIX A

For the measurement of the voltage U with the DVM the running average $\overline{U}_N$ after N measurements is

$$\overline{U}_N = [(N-1)\overline{U}_{N-1} + U_N]/N ,$$

and the dispersion is estimated by

$$\sigma_N = \left[\sum_{i=1}^{N} (U_i - \overline{U}_i)^2/(N-1)\right]^{1/2} .$$

This equation for σ is very similar to the exact calculation where $\overline{U}_N$ would have been used instead of $\overline{U}_i$.

APPENDIX B

The means and medians are calculated by

$$\text{Mean} = \left(\sum_{i=1}^{n} iC_i\right) \Big/ \sum_{i=1}^{n} C_i ,$$

where C_i is the number of counts in channel i, and n is the number of channels across the peak:

$$\text{Median} = 0.5 + m + (S_{1/2} - S_m)/(S_{m+1} - S_m) ,$$

where $S_{1/2} = \frac{1}{2}\sum_{i=1}^{n} C_i$ and $S_m = \sum_{i=1}^{m} C_i$, with m such that $S_m \leq S_{1/2} < S_{m+1}$.

---

*Permanent address: Lawrence Berkeley Laboratory, Berkeley, California.
†Permanent address: Institut de Physique Corpusculaire Université de Louvain, Louvain-la-Neuve, Belgium.
‡France-Quebec postdoctoral fellow 1972–1973. Present address: Foster Radiation Laboratory, McGill University, Montreal, Canada.
§Permanent address: Gesellschaft für Schwerionenforschung mbH, Darmstadt, Germany.

[1]J. D. Bowman, A. M. Poskanzer, R. G. Korteling, and G. W. Butler, Phys. Rev. C 9, 836 (1974), and references therein.
[2]R. Klapisch, C. Thibault, A. M. Poskanzer, R. Prieels, C. Rigaud, and E. Roeckl, Phys. Rev. Lett. 29, 1254 (1972), and references therein.
[3]A. G. Artukh, V. V. Avdeichikov, G. F. Gridnev, V. L. Mikheev, V. V. Volkov, and J. Wilczynski, Nucl. Phys. A176, 284 (1971).
[4]G. T. Garvey, W. J. Gerace, R. L. Jaffe, I. Talmi, and I. Kelson, Rev. Mod. Phys. Suppl. 41, 1 (1969).
[5]C. Thibault and R. Klapisch, Phys. Rev. C 9, 793 (1974).
[6]J. D. Bowman, A. M. Poskanzer, R. G. Korteling, and G. W. Butler, Phys. Rev. Lett. 31, 614 (1973).
[7]R. Klapisch, C. Thibault-Philippe, C. Détraz, J. Chaumont, R. Bernas, and E. Beck, Phys. Rev. Lett. 23, 652 (1969).
[8]A. G. Artukh, G. F. Gridnev, V. L. Mikheev, V. V. Volkov, and J. Wilczynski, Nucl. Phys. A192, 170 (1972).
[9]R. Klapisch, R. Prieels, C. Thibault, A. M. Poskanzer, C. Rigaud, and E. Roeckl, Phys. Rev. Lett. 31, 118 (1973).
[10]D. R. Goosman and D. E. Alburger, Phys. Rev. C 10, 756 (1974).
[11]E. Roeckl, P. F. Dittner, C. Détraz, R. Klapisch, C. Thibault, and C. Rigaud, Phys. Rev. C 10, 1181 (1974).
[12]J. Cerny, S. W. Cosper, G. W. Butler, R. H. Pehl, F. S. Goulding, D. A. Landis, and C. Détraz, Phys. Rev. Lett. 16, 469 (1966).
[13]A. M. Poskanzer, R. A. Esterlund, and R. McPherson, Phys. Rev. Lett. 15, 1030 (1965).
[14]K. H. Wilcox, N. A. Jelley, G. J. Wozniak, R. B. Weisenmiller, H. L. Harney, and J. Cerny, Phys. Rev. Lett. 30, 866 (1973).
[15]G. C. Ball, G. J. Costa, W. G. Davies, J. S. Forster, J. C. Hardy, and A. B. McDonald, Phys. Rev. Lett. 31, 395 (1973).
[16]G. C. Ball, W. G. Davies, J. S. Forster, and J. C. Hardy, Phys. Rev. Lett. 28, 1069, 1497 (1972).
[17]E. R. Flynn and J. D. Garrett, Phys. Rev. C 9, 210 (1974).
[18]D. R. Goosman, D. E. Alburger, and J. C. Hardy, Phys. Rev. C 7, 1133 (1973).
[19]D. E. Alburger, D. R. Goosman, and C. N. Davids, Phys. Rev. C 8, 1011 (1973).
[20]D. R. Goosman, C. N. Davids, and D. E. Alburger, Phys. Rev. C 8, 1331 (1973).
[21]D. R. Goosman and D. E. Alburger, Phys. Rev. C 7, 2409 (1973).
[22]D. R. Goosman and D. E. Alburger, Phys. Rev. C 6, 825 (1972); D. R. Goosman, C. N. Davids, and D. E. Alburger *ibid.* 8, 1324 (1973).
[23]D. R. Goosman and D. E. Alburger, Phys. Rev. C 6, 820 (1972).
[24]R. Klapisch, C. Thibault, C. Rigaud, A. M. Poskanzer, L. Lessard, and W. Reisdorf, in *Proceedings of the International Conference on Nuclear Physics, Munich, Germany, 1973,* edited by J. de Boer and H. J. Mang (North-Holland, Amsterdam/American Elsevier, New York, 1974), Vol. 1, p. 325.

[25]R. Klapisch, J. Chaumont, C. Philippe, I. Amarel, R. Fergeau, M. Salomé, and R. Bernas, Nucl. Instrum. Methods 53, 216 (1967).
[26]C. Thibault, Ph.D. thesis, Orsay, 1971 (unpublished).
[27]C. Rigaud, Thèse de 3e cycle, Orsay, 1972 (unpublished).
[28]R. Klapisch *et al.* (unpublished).
[29]J. M. Maugain, CERN Report No. NPA Int. 6722, 1967 (unpublished).
[30]F. J. M. Farley and B. S. Carter, Nucl. Instrum. Methods, 28, 279 (1964).
[31]W. H. Johnson Jr., in Proceedings of the International Conference on the Properties of Nuclei Far From the Region of Beta-Stability, Leysin, Switzerland, 1970 [CERN Report No. CERN 70-30, 1970 (unpublished)], p. 307.
[32]A. M. Wapstra and N. B. Gove, Nucl. Data A9, 267 (1971).
[33]A. M. Poskanzer, S. W. Cosper, E. K. Hyde, and J. Cerny, Phys. Rev. Lett. 17, 1271 (1966).
[34]J. P. Deutsch, L. Grenacs, J. Lehmann, P. Lipnik, and P. C. Macq, Phys. Lett. 28B, 178 (1968); D. L. Auton, B. Zeidman, H. T. Fortune, J. P. Schiffer, and R. C. Bearse, Bull. Am. Phys. Soc. 14, 489 (1969).
[35]S. W. Cosper, J. Cerny, and R. C. Gatti, Phys. Rev. 154, 1193 (1967).
[36]S. Cohen and D. Kurath, Nucl. Phys. 73, 1 (1965); D. Kurath, private communication to C. Dêtraz.
[37]P. Goldhammer, J. R. Hill, and J. Nachamkin, Nucl. Phys. A106, 62 (1968); and private communication to C. Thibault.
[38]G. Hock, private communication to R. Klapisch; A. N. Boĭarkina, Izv. Akad. Nauk SSSR Ser. Fiz. 28, 337 (1964) [Bull. Acad. Sci. USSR Phys. Ser. 28, 255 (1965)].
[39]W. D. Myers and W. J. Swiatecki, University of California Lawrence Radiation Laboratory Report No. UCRL 11980, 1965, (unpublished), and Nucl. Phys. 81, 1 (1966).
[40]W. D. Myers and W. J. Swiatecki, University of California Lawrence Radiation Laboratory, Report No. UCRL 19543, 1970 (unpublished); Report No. LBL 1957, 1973 (unpublished); and W. M. Howard and J. R. Nix, University of California Los Alamos Scientific Laboratory Report No. LA-UR-73-972, 1973 (unpublished).
[41]P. A. Seeger and W. M. Howard, University of California Los Alamos Scientific Laboratory Report No. LA-5750 (unpublished).
[42]B. J. Cole, A. Watt, and R. R. Whitehead, University of Glasgow, Glasgow, Scotland, Report No. G.U. 24 (unpublished).
[43]T. T. S. Kuo, Nucl. Phys. A103, 71 (1967).
[44]B. M. Preedom and B. H. Wildenthal, Phys. Rev. C 6, 1633 (1972).
[45]N. A. Jelley, J. Cerny, D. P. Stahel, and K. H. Wilcox, University of California Lawrence Berkeley Laboratory Report No. LBL-3414, 1974 (unpublished).
[46]X. Campi, H. Flocard, A. Kerman, and S. Koonin (unpublished).
[47]One should also point out that the total binding energies calculated by Ref. 46 contain spurious terms dependent on the parity of N and Z which are understood but have not yet been eliminated. The effect of these spurious terms is minimized, however, when looking at differences between isotopes of the same parity in neutron number; such is the case with E_{2N} in Fig. 10.